

## Article

# Calcium signaling in endocardial and epicardial ventricular myocytes from streptozotocin-induced diabetic rats

Al Kury, Lina T., Sydorenko, Vadym, Smail, Manal MA, Qureshi, Muhammad A., Shmygol, Anatoly, Papandreou, Dimitrios and Singh, Jaipaul

Available at <http://clock.uclan.ac.uk/35309/>

*Al Kury, Lina T., Sydorenko, Vadym, Smail, Manal MA, Qureshi, Muhammad A., Shmygol, Anatoly, Papandreou, Dimitrios and Singh, Jaipaul ORCID: 0000-0002-3200-3949 (2021) Calcium signaling in endocardial and epicardial ventricular myocytes from streptozotocin-induced diabetic rats. Journal of Diabetes Investigation, 12 (4). pp. 493-500. ISSN 2040-1116*

It is advisable to refer to the publisher's version if you intend to cite from the work.  
<http://dx.doi.org/10.1111/jdi.13451>

For more information about UCLan's research in this area go to  
<http://www.uclan.ac.uk/researchgroups/> and search for <name of research Group>.

For information about Research generally at UCLan please go to  
<http://www.uclan.ac.uk/research/>

All outputs in CLoK are protected by Intellectual Property Rights law, including Copyright law. Copyright, IPR and Moral Rights for the works on this site are retained by the individual authors and/or other copyright owners. Terms and conditions for use of this material are defined in the [policies](#) page.

# Calcium signaling in endocardial and epicardial ventricular myocytes from streptozotocin-induced diabetic rats

Lina T Al Kury<sup>1\*</sup>, Vadym Sydorenko<sup>2</sup>, Manal MA Smail<sup>3</sup>, Muhammad A Qureshi<sup>3</sup>, Anatoly Shmygol<sup>3</sup>, Dimitrios Papandreou<sup>1</sup>, Jaipaul Singh<sup>4</sup>, Frank Christopher Howarth<sup>3</sup>

<sup>1</sup>Department of Health Sciences, College of Natural and Health Sciences, Zayed University, Abu Dhabi, United Arab Emirates, <sup>2</sup>Department of Cellular Membranology, Bogomoletz Institute of Physiology, Kiev, Ukraine, <sup>3</sup>Department of Physiology, College of Medicine and Health Sciences, UAE University, Al Ain, United Arab Emirates, and <sup>4</sup>School of Forensic and Applied Sciences, University of Central Lancashire, Preston, UK

## Keywords

Ca<sup>2+</sup> transients, Na<sup>+</sup>/Ca<sup>2+</sup> exchanger, Streptozotocin-induced diabetes

## \*Correspondence

Lina T Al Kury  
Tel.: +971-50-662-3975  
Fax: +971-2-443-4847  
E-mail address:  
lina.alkury@zu.ac.ae

*J Diabetes Investig* 2020

doi: 10.1111/jdi.13451

## ABSTRACT

**Aims/Introduction:** Abnormalities in Ca<sup>2+</sup> signaling have a key role in hemodynamic dysfunction in diabetic heart. The purpose of this study was to explore the effects of streptozotocin (STZ)-induced diabetes on Ca<sup>2+</sup> signaling in epicardial (EPI) and endocardial (ENDO) cells of the left ventricle after 5–6 months of STZ injection.

**Materials and Methods:** Whole-cell patch clamp was used to measure the L-type Ca<sup>2+</sup> channel (LTCC) and Na<sup>+</sup>/Ca<sup>2+</sup> exchanger currents. Fluorescence photometry techniques were used to measure intracellular free Ca<sup>2+</sup> concentration.

**Results:** Although the LTCC current was not significantly altered, the amplitude of Ca<sup>2+</sup> transients increased significantly in EPI-STZ and ENDO-STZ compared with controls. Time to peak LTCC current, time to peak Ca<sup>2+</sup> transient, time to half decay of LTCC current and time to half decay of Ca<sup>2+</sup> transients were not significantly changed in EPI-STZ and ENDO-STZ myocytes compared with controls. The Na<sup>+</sup>/Ca<sup>2+</sup> exchanger current was significantly smaller in EPI-STZ and in ENDO-STZ compared with controls.

**Conclusions:** STZ-induced diabetes resulted in an increase in amplitude of Ca<sup>2+</sup> transients in EPI and ENDO myocytes that was independent of the LTCC current. Such an effect can be attributed, at least in part, to the dysfunction of the Na<sup>+</sup>/Ca<sup>2+</sup> exchanger. Additional studies are warranted to improve our understanding of the regional impact of diabetes on Ca<sup>2+</sup> signaling, which will facilitate the discovery of new targeted treatments for diabetic cardiomyopathy.

## INTRODUCTION

Cardiac contractility is controlled by variations in the concentration of intracellular free Ca<sup>2+</sup>. During the process of excitation–contraction coupling, depolarization of the ventricular myocyte causes the opening of L-type Ca<sup>2+</sup> channel (LTCCs) and the influx of small amounts of Ca<sup>2+</sup> into the cardiac cells. This influx of Ca<sup>2+</sup> stimulates a large release of Ca<sup>2+</sup> (Ca<sup>2+</sup> transient) from the sarcoplasmic reticulum (SR) through the ryanodine receptors (RyR) resulting in a transient rise of intracellular Ca<sup>2+</sup> (Ca<sup>2+</sup> transient). Ca<sup>2+</sup> attaches to troponin C, which initiates and regulates the process of myocyte contraction. During the process of

myocyte relaxation, Ca<sup>2+</sup> is removed from the cytoplasm through four main pathways: (i) the uptake of Ca<sup>2+</sup> into the SR through SR Ca<sup>2+</sup>-ATPase (SERCA pump); (ii) efflux of Ca<sup>2+</sup> from the cell primarily through the Na<sup>+</sup>/Ca<sup>2+</sup> exchanger (NCX); and (iii) to a lesser extent the Ca<sup>2+</sup>-ATPase in the plasma membrane<sup>1</sup>; and (iv) also uptake of Ca<sup>2+</sup> by the mitochondria<sup>2,3</sup>.

Disturbances in the mechanism(s) of Ca<sup>2+</sup> signaling will inevitably have implications for cardiac myocyte contraction. Previous studies of left ventricle cells obtained from the STZ-treated rat have shown alterations in the Ca<sup>2+</sup> transient, including prolonged TPK<sup>4,5</sup>, prolonged THALF relaxation<sup>6</sup> and unaltered<sup>7</sup> or reduced<sup>8</sup> amplitude of Ca<sup>2+</sup> transient. These alterations in Ca<sup>2+</sup> transient might be attributed variously to diminished SR Ca<sup>2+</sup> content, release and uptake<sup>9–11</sup>, reduced activity of L-type Ca<sup>2+</sup> channel<sup>12–14</sup> and NCX<sup>7,13</sup>.

Received 19 August 2020; revised 8 October 2020; accepted 22 October 2020

Supporting these findings, earlier studies of STZ-treated rats variously reported reduced cardiac output, fractional shortening and ejection fraction<sup>4,14,15</sup>. In cardiac cells isolated from STZ-treated rat, there was a prolonged time course of shortening<sup>6,16,17</sup>, frequently prolonged relaxation<sup>4,16</sup>, and slowed velocity of shortening and re-lengthening<sup>14</sup>. Studies also showed either no significant change<sup>6,12</sup> or reduction<sup>14</sup> in the amplitude of shortening. These different results could be partly attributed to the duration of diabetes or the methodology used in the experiments.

It is well known that the electromechanical characteristics of cardiac cells across the ventricular walls are different. This heterogeneity is partly attributed to distinctive expression of different ion channels and associated ionic currents that lead to variation in action potential waveforms seen in epicardial (EPI), midmyocardial and endocardial (ENDO) cells<sup>18–20</sup>. For example, *in vivo* echocardiographic studies in rat ventricular myocardium have shown that layers of the epicardium contract less and slower than the layers of the subendocardium<sup>21</sup>. It is important to highlight that any disruption in the differential distribution of ion channels responsible for  $\text{Ca}^{2+}$  transport across the walls of the ventricles is expected to be involved in the dysfunction of cardiac cells in disease<sup>7,15,22,23</sup>. Earlier work in spontaneously hypertensive rats has shown a transmurally altered time course and amplitude of action potential, variation in  $\text{Ca}^{2+}$  transients, and contraction in sub-EPI and sub-ENDO myocytes during compensated hypertrophy<sup>24</sup>. Transmural alteration in the activity of NCX,  $\text{Ca}^{2+}$  content of the SR and amplitude of  $\text{Ca}^{2+}$  transient have also been shown in an earlier study in spontaneously hypertensive rat<sup>25</sup>.

To date, only a few studies have explored the transmural effect of STZ-induced diabetes on  $\text{Ca}^{2+}$  signaling in ventricular myocytes<sup>26–28</sup>. For this reason, the current work was undertaken to investigate the progressive regional effects of diabetes on ventricular myocytes. To the best of our knowledge, this is the first study to investigate the effects of STZ-induced diabetes on LTCC current simultaneously measured with  $\text{Ca}^{2+}$  transients. Previous experiments generally measured LTCC current and  $\text{Ca}^{2+}$  transient in separate experiments. The influx of  $\text{Ca}^{2+}$  through LTCCs is inextricably linked to the release of  $\text{Ca}^{2+}$  from the SR ( $\text{Ca}^{2+}$ -induced  $\text{Ca}^{2+}$  release). Therefore, this study has investigated the effects of STZ-induced diabetes on LTCC current simultaneously measured with intracellular  $\text{Ca}^{2+}$ , and also NCX current in EPI and ENDO ventricular myocytes from rats 5–6 months after the induction of diabetes.

## METHODS

### Experimental model

Experiments were carried out in STZ-induced diabetic rats<sup>29,30</sup>. A single intraperitoneal injection of STZ (60 mg/kg body-weight) in citrate buffer was used to induce diabetes in young adult (220–250 g) male Wistar rats. Age-matched control animals were injected with citrate buffer alone. Rats were kept in a 12/12 h light/dark cycle. Food and water were supplied

ad libitum. Both the control and experimental groups received standard pelleted rat chow.

Before each experiment, body and heart weights, in addition to non-fasting blood glucose level (One Touch Ultra, LifeScan Inc., Milpitas, CA, USA) were measured. All experiments were carried out 5–6 months after treatment with STZ in ENDO and EPI myocytes. Ethical approval of the work was received from the UAE University Animal Research Ethics Committee (UAE University, A11-15, 2015). All experiments were carried out according to the institution guidelines.

### Isolation of ventricular myocytes

Ventricular myocytes were obtained by enzymatic and mechanical dispersal techniques in accordance with previously described protocols<sup>24,27,28</sup>. Animals were euthanized with a guilotine. Hearts were isolated, mounted on a Langendorff system for retrograde perfusion and perfused at 36–37°C with a cell isolation solution (see Appendix S1)<sup>27</sup>. The perfusion flow rate was 8 mL/g heart<sup>-1</sup>.min<sup>-1</sup>. On stabilization of heart contraction, perfusion was switched to  $\text{Ca}^{2+}$ -free cell isolation solution containing egtazic acid (0.1 mmol/L) for 4 min, and then to cell isolation solution containing  $\text{Ca}^{2+}$  (0.05 mmol/L), type 1 collagenase (0.60 mg/mL) and type XIV protease (0.075 mg/mL) for 6 min. On completion of enzymatic treatment, hearts were detached from the Langendorff perfusion system and the left ventricle was further dissected as described in earlier studies<sup>27,28</sup>. Thin sections were carefully dissected by fine scissors from the outermost layer (EPI) and innermost layer (ENDO) of the left ventricle. The sections were gently minced and shaken in an isolation solution containing collagenase and 1% bovine serum albumin. Cells were then filtered at 4-min intervals and re-suspended in cell isolation solution that contained 0.75 mmol/L  $\text{Ca}^{2+}$ .

### Simultaneous recording of L-type $\text{Ca}^{2+}$ current and $\text{Ca}^{2+}$ transient

Simultaneous recording of LTCC current and  $\text{Ca}^{2+}$  transients were measured in EPI and ENDO ventricular cells according to modifications of previously described methods<sup>27,28,31</sup>. All experiments were carried out at 34°C. LTCC current was measured with an Axopatch 200B amplifier (Molecular Devices, Sunnyvale, CA, USA). Analog signal was filtered using a four-pole Bessel filter (bandwidth of 5 kHz), and digitized at a sampling rate of 10 kHz using a Digidata 1550 digitizer (Molecular Devices). The voltage clamp protocols and data acquisition were controlled by WinWCP 4.05 software (Strathclyde Electrophysiology Software, Glasgow, UK). Patch pipettes were made from filamented borosilicate glass. Resistance of electrodes was 2–4 MΩ. Seal resistances were 1–5 GΩ. A current–voltage (I–V) relationship was achieved by the application of 300 ms test pulses (–30 to +50 mV) in 10 mV steps from a holding potential of –40 mV. Intracellular  $\text{Ca}^{2+}$  recordings were obtained by loading the cells with 30 μmol/L fura-2-pentapotassium salt through the patch pipette for 5 min, and

excited at 360- and 380-nm wavelengths with dual LED light source, controlled by a spectrophotometry unit at 100 Hz. The fluorescence signal at 510 nm was collected through an adjustable diaphragm and a photomultiplier tube. WinWCP 4.05 software was used to sample signals at 10 kHz. All data were stored on a computer for subsequent analysis. After the subtraction of background signal, fluorescent signals were recorded as  $F_{360}/F_{380}$  (ratio of the fluorescent intensity when excited at 360 nm [ $F_{360}$ ] to that when excited at 380 nm [ $F_{380}$ ] and expressed as a ratio unit). The whole-cell bath solution and pipette solution used are described in the Appendix S1.

### Measurement of $\text{Na}^+/\text{Ca}^{2+}$ exchange current

The NCX current was recorded according to modifications of previously described techniques<sup>31</sup>. Experiments were carried out at 34°C. Recording of the NCX current was obtained with an Axopatch 200B amplifier using a voltage ramp protocol. Cells were held at a holding potential of -40 mV. Voltage ramps were deployed at a steady rate of 0.1 V/s from +60 mV to -100 mV. Resistance of electrodes was 3–5 MΩ. Seal resistances were 1–5 GΩ. Oubain (100 μmol/L), nifedipine (10 μmol/L) and niflumic acid (30 μmol/L) were used to block  $\text{Na}^+/\text{K}^+/\text{ATPase}$ ,  $\text{Ca}^{2+}$  and  $\text{Cl}^-$  currents, respectively. Nickel chloride solution (10 mmol/L) was used to block NCX. The NCX current was measured as the current sensitive to nickel ( $\text{Ni}^{2+}$ ). NCX current was isolated by subtracting  $\text{Ni}^{2+}$ -insensitive component from the total current<sup>31</sup>. Whole-cell bath solution and pipette solution used are described in Appendix S1.

### Statistical analysis

Results were represented as mean ± standard error of the mean of “*n*” observations. As appropriate, independent samples *t*-test or one-way ANOVA followed by Bonferroni corrected *t*-tests were used for statistical comparisons. A *P*-value <0.05 was considered significant.

## RESULTS

### General characteristics

Bodyweight and heart weight were significantly reduced ( $P < 0.05$ ) in STZ-pretreated diabetic rats. In comparison with their respective age-matched controls, heart weight/bodyweight

**Table 1** | General characteristics of streptozotocin-induced diabetic and age-matched control rats

	Control	Streptozotocin
Bodyweight (g)	417.3 ± 9.9	274.2 ± 8.6 <sup>†</sup>
Heart weight (g)	1.45 ± 0.03	1.28 ± 0.03 <sup>†</sup>
Heart weight/bodyweight (mg/g)	3.50 ± 0.07	4.68 ± 0.10 <sup>†</sup>
Non-fasting blood glucose (mg/dL)	83.3 ± 1.31	483.9 ± 20.2 <sup>†</sup>

Data are the mean ± standard error of the mean, *n* = 15–17 rats.

<sup>†</sup>*P* < 0.05 for diabetic compared with controls.

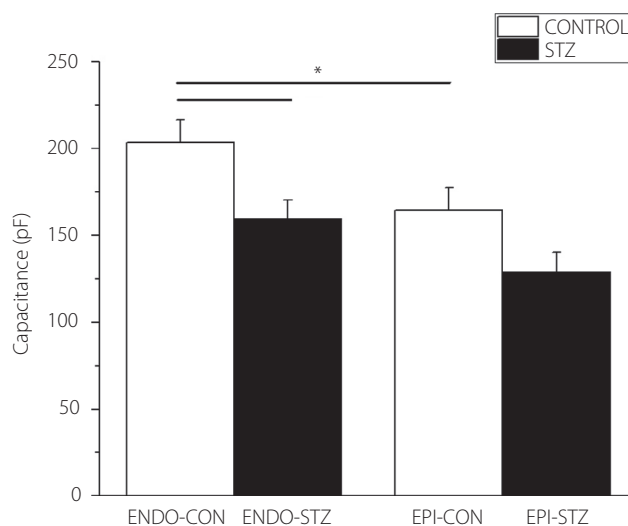


**Figure 1** | Mean cell capacitance in endocardial control (ENDO-CON), endocardial streptozotocin (STZ)-pretreated (ENDO-STZ), epicardial control (EPI-CON) and epicardial streptozotocin-pretreated (EPI-STZ) myocytes. Data are the mean ± standard error of the mean, *n* = 13–17 cells from 10–14 hearts; \**P* < 0.05.

and non-fasting blood glucose were greater in STZ-pretreated diabetic rats (Table 1).

### Cell capacitance

Cell capacitance was significantly lower in ENDO-STZ compared with ENDO-CON ventricular cells ( $P < 0.05$ ; Figure 1). There was a small variation in cell capacitance between EPI-STZ and EPI-CON myocytes; however, the variation was not significant ( $P > 0.05$ ).

### L-type $\text{Ca}^{2+}$ current and $\text{Ca}^{2+}$ transient

Typical tracings of LTCC current and  $\text{Ca}^{2+}$  transients measured at 0 mV test potential are shown in Figure 2a. The mean current–voltage (*I/V*) relationships of the LTCC current for ENDO-STZ, ENDO-CON, EPI-STZ and EPI-CON ventricular cells are shown in Figure 2b, and the currents generated at 0 mV test voltage are represented in Figure 2c. LTCC current amplitudes were not significantly ( $P > 0.05$ ) different in ENDO-STZ and EPI-STZ compared with their respective controls at 0 mV (Figure 2c).  $\text{Ca}^{2+}$  transient fura-2 ratio-voltage relationship for ENDO-STZ, ENDO-CON, EPI-STZ and EPI-CON ventricular myocytes are represented in Figure 2d.  $\text{Ca}^{2+}$  transients generated at 0 mV are represented in Figure 2e. The amplitude of  $\text{Ca}^{2+}$  transients were significantly ( $P < 0.05$ ) larger in ENDO-STZ and EPI-STZ compared with their controls (Figure 2e). TPK LTCC current (Figure 2f) and TPK  $\text{Ca}^{2+}$  transient (Figure 2g) were not significantly ( $P > 0.05$ ) different in ENDO-STZ and EPI-STZ compared with their respective controls ( $P > 0.05$ ). THALF decay of LTCC current (Figure 2h) and THALF decay of the  $\text{Ca}^{2+}$

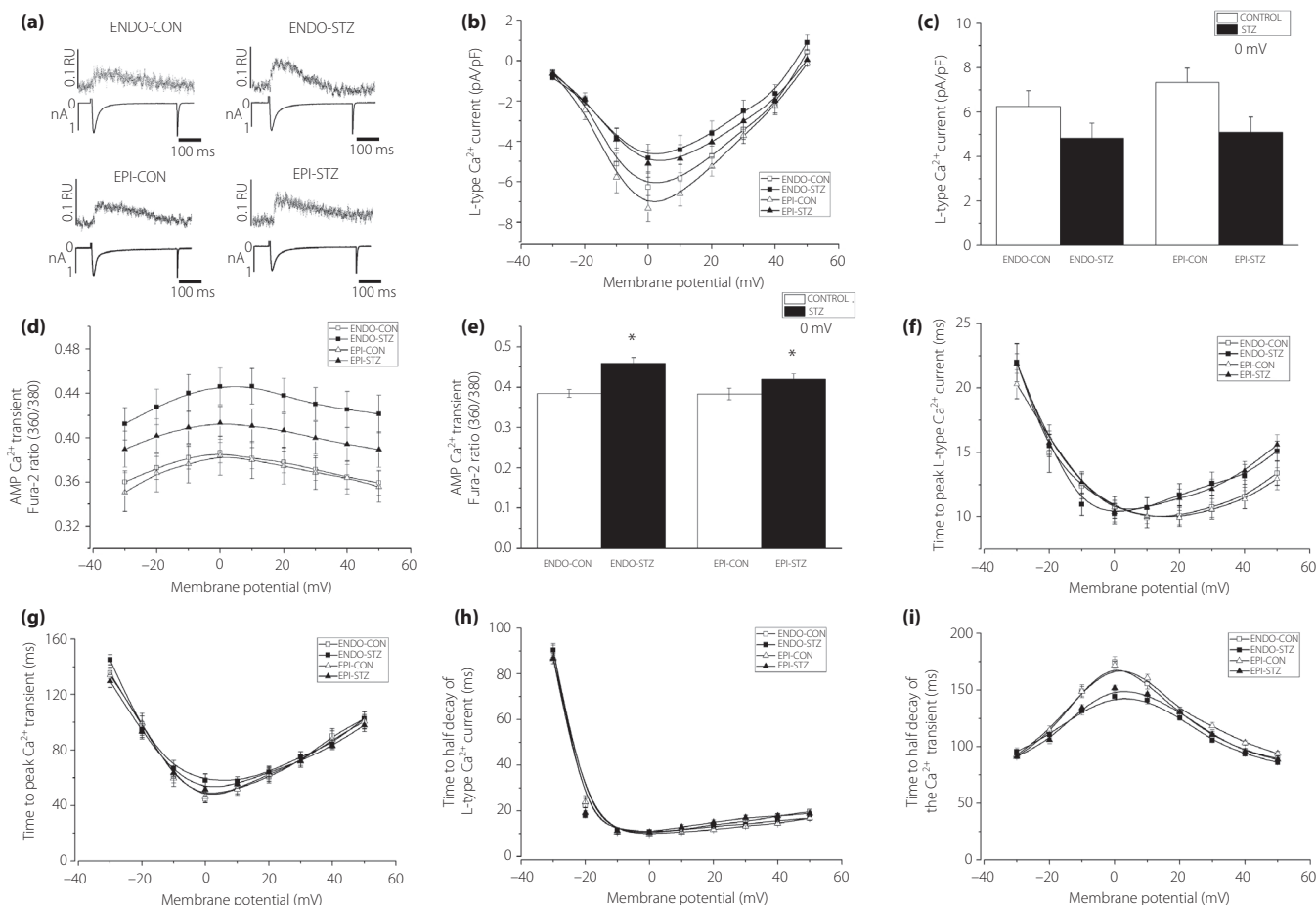


**Figure 2** | L-type  $\text{Ca}^{2+}$  channel (LTCC) current and  $\text{Ca}^{2+}$  transient in endocardial control (ENDO-CON), endocardial streptozotocin (STZ)-pretreated (ENDO-STZ), epicardial control (EPI-CON) and epicardial streptozotocin-pretreated (EPI-STZ) myocytes. (a) Typical recordings of LTCC current and  $\text{Ca}^{2+}$  transient at a test potential of 0 mV. (b) Mean recordings of LTCC current at test voltages in the range  $-30$  to  $+50$  mV. (c) Mean LTCC current at a test voltage of 0 mV. (d) Mean recordings of amplitude (AMP) of  $\text{Ca}^{2+}$  transients at test voltages in the range  $-30$  to  $+50$  mV. (e) Mean AMP of  $\text{Ca}^{2+}$  transients at a test potential of 0 mV. (f) TPK of LTCC current at test potentials in the range  $-30$  to  $+50$  mV. (g) TPK of  $\text{Ca}^{2+}$  transients at test potentials in the range  $-30$  to  $+50$  mmol/L. (h) Time to half decay of LTCC current at test potentials in the range  $-30$  to  $+50$  mV. (i) Time to half of  $\text{Ca}^{2+}$  transients at test potentials in the range  $-30$  to  $+50$  mV. Data are the mean  $\pm$  standard error of the mean,  $n = 13$ – $16$  cells from 12–14 hearts;  $*P < 0.05$ .

transient (Figure 2i) were not significantly ( $P < 0.05$ ) different in ENDO-STZ and EPI-STZ compared with their respective controls.

### $\text{Na}^+/\text{Ca}^{2+}$ exchange current

The current of NCX was recorded by applying a voltage ramp between  $+60$  and  $-100$  mV. The NCX current was calculated as the difference between the current generated in the presence of  $10 \mu\text{mol/L}$  nifedipine and the current in the presence of nifedipine and  $10 \text{ mmol/L}$   $\text{Ni}^{2+}$ . Mean recordings of the ramp current in ENDO-CON, ENDO-STZ, EPI-CON and EPI-STZ ventricular cells are represented in Figure 3a. At  $+60$  mV, the amplitude of the NCX current was significantly ( $P < 0.05$ ) smaller in ENDO-STZ and in EPI-STZ compared with their respective controls ( $P < 0.05$ ) (Figure 3b). Similarly, at  $-$

$100$  mV, the amplitude of the NCX current was significantly ( $P < 0.05$ ) smaller in ENDO-STZ and EPI-STZ compared with their respective controls (Figure 3c).

### DISCUSSION

The findings of the present study show that STZ-induced diabetes causes significant alteration in  $\text{Ca}^{2+}$  transients and NCX current in EPI and ENDO ventricular myocytes. To the best of our knowledge, this is the first study to investigate the regional effects of STZ-induced diabetes on LTCC current simultaneously measured with  $\text{Ca}^{2+}$  transients and NCX current in ventricular myocytes from STZ-induced diabetic rat.

Many changes during excitation–contraction coupling might give rise to changes in the  $\text{Ca}^{2+}$  transient. In our experiments,

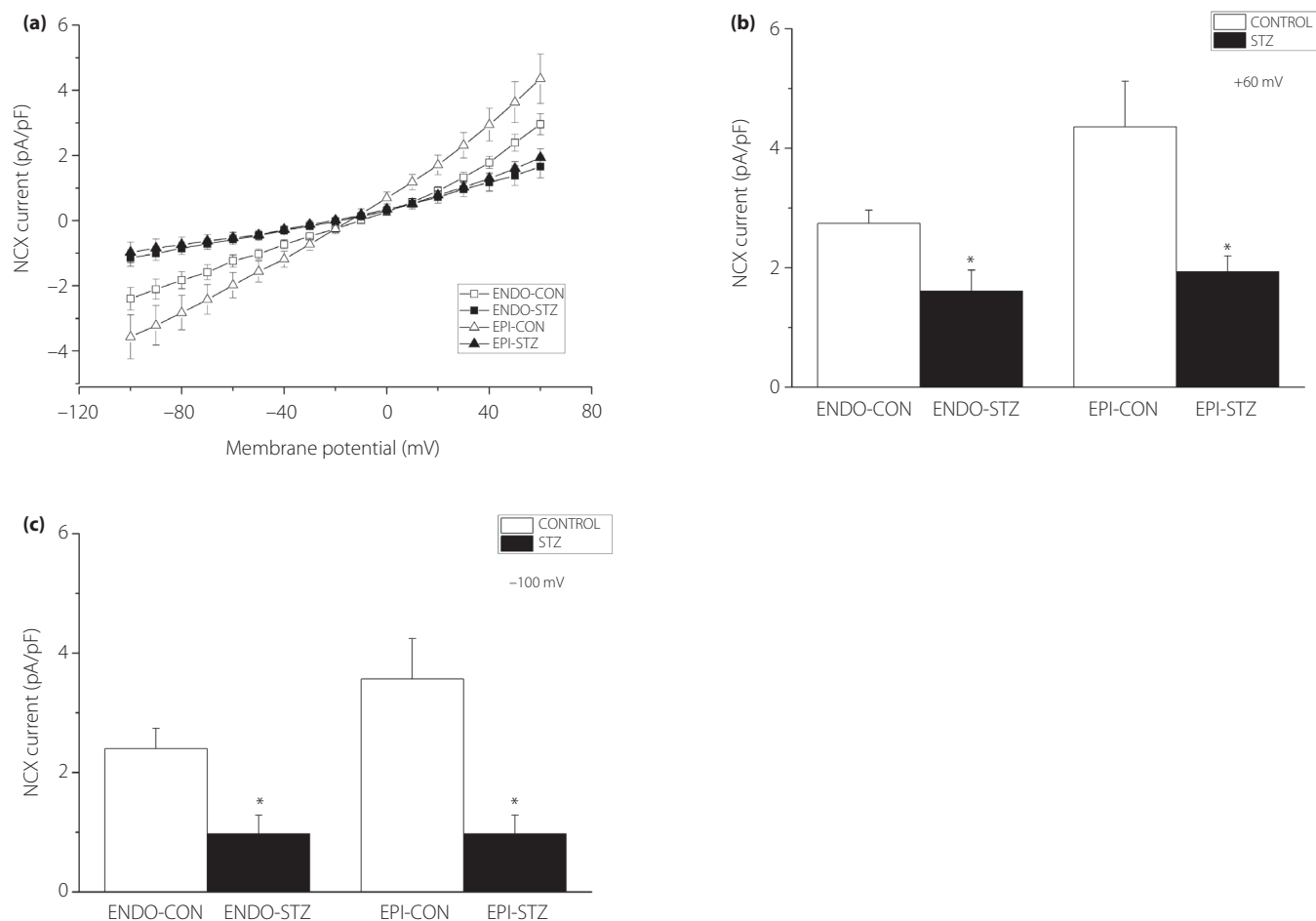


**Figure 3** | Na<sup>+</sup>/Ca<sup>2+</sup> exchange current in endocardial control (ENDO-CON), endocardial streptozotocin (STZ)-pretreated (ENDO-STZ), epicardial control (EPI-CON) and epicardial streptozotocin-pretreated (EPI-STZ) myocytes. (a) Mean recordings of Na<sup>+</sup>/Ca<sup>2+</sup> exchange current in (range -100 to +60 mV). (b) Mean peak currents of Na<sup>+</sup>/Ca<sup>2+</sup> exchange current at +60 mV. (c) Mean peak currents of Na<sup>+</sup>/Ca<sup>2+</sup> exchange current at -100 mV. Data are the mean  $\pm$  standard error of the mean,  $n = 14$ –17 cells from 9–11 hearts. \* $P < 0.05$ . NCX, Na<sup>+</sup>/Ca<sup>2+</sup> exchanger.

the amplitude and the kinetics of the LTCC current were similar in rat ventricular cells from EPI compared with ENDO regions. The amplitude of LTCC currents were not significantly different in ENDO-STZ and EPI-STZ ventricular cells compared with their controls. Although some studies have previously reported decreased amplitude<sup>12,32</sup>, many studies have reported no change in LTCC currents in ventricular cells from STZ-treated rat<sup>4,11,33,34</sup>.

Interestingly, the amplitude of the Ca<sup>2+</sup> transients were significantly larger in EPI-STZ and ENDO-STZ myocytes compared with their respective controls. However, no regional difference in Ca<sup>2+</sup> transients was observed. Earlier studies reported either reduced<sup>4,15,35</sup> or unaltered<sup>16,32,36</sup> Ca<sup>2+</sup> transients in ventricular cells, isolated from STZ-induced diabetic animals. In comparison with other studies, in which Ca<sup>2+</sup> transients were measured after 3–12 weeks of STZ treatment<sup>16,17,32,33,37</sup>, the present experiments were carried out in EPI and ENDO ventricular myocytes 5–6 months after STZ treatment. Thus, the variation in results

might be partly related to the degree of progression of diabetes. Furthermore, the discrepancy between the present data and other results, where decreased amplitude<sup>38</sup> or no change in amplitude<sup>7</sup> of the Ca<sup>2+</sup> transients were observed, might be down to the fact that different Ca<sup>2+</sup> dyes were used for intracellular Ca<sup>2+</sup> recordings. In the present study, a low concentration of fura-2-pentapotassium salt was dialyzed into the cell through the patch pipette. However, other studies<sup>7,38</sup> used ester of Indo-1 to load the indicator. Although both are high affinity indicators that have been used for cytosolic Ca<sup>2+</sup> measurements in many studies in cardiac myocytes and other cell types, variation in indicator and/or loading technique might account for different results. For example, the use of ester of Indo-1 dye is sometimes associated with overloading of cytoplasm with Ca<sup>2+</sup> indicator leading to increased buffering of Ca<sup>2+</sup>, slowing down the transients' decay and reducing their amplitude.

The observed rise in the amplitudes of Ca<sup>2+</sup> transients is explained by changes in pathways of Ca<sup>2+</sup> extrusion (e.g.,



NCX) which, along with SERCA, are responsible for decreasing cytosolic  $\text{Ca}^{2+}$ . In the present study, there was a significant decrease in NCX current in both EPI and ENDO ventricular cells, although no regional difference in the activity of NCX was observed. Earlier studies have also shown that the density of NCX current was reduced<sup>7,13,39</sup> and current inactivation was prolonged<sup>13</sup> in ventricular cells isolated from STZ-treated diabetic rats. These variations in the amplitude and kinetics of current were accompanied with decreased NCX messenger ribonucleic acid (mRNA)<sup>7</sup> and reduced or unaltered NCX protein in STZ-induced diabetic rat heart<sup>8,11,40</sup>. It is possible that the decrease in the  $\text{Ca}^{2+}$  extrusion rate through NCX leads to a net increase in intracellular  $\text{Ca}^{2+}$ , increase in SR  $\text{Ca}^{2+}$  load and, as a consequence, increased cytosolic  $\text{Ca}^{2+}$  transients<sup>11,14,17,33,42</sup>. Alternatively, the increase in the amplitude of  $\text{Ca}^{2+}$  transients can be linked to RyR dysfunction. Abnormal function of RyR is associated with various diseases, including cardiac hypertrophy and STZ-induced type 1 diabetes<sup>43</sup>. It is known that the metabolic changes associated with diabetes stimulate the production of reactive oxygen species. As RyR structure is rich in free thiol groups, it is subject to oxidative stress, changing its tertiary structure and altering its sensitivity to  $\text{Ca}^{2+}$ <sup>43,44</sup>. In an earlier study in 7-week sedentary type 1 diabetic rats, the frequency of  $\text{Ca}^{2+}$  spark was threefold higher, and evoked release of  $\text{Ca}^{2+}$  was dys-synchronous with the diastolic release. Although the steady-state RyR protein was not altered, its response to  $\text{Ca}^{2+}$  was changed. The RyR also showed an approximately 1.5-fold rise in phosphorylation at Ser 2808 and Ser 2814 residues<sup>14</sup>.

In addition to the effects observed in diabetes, earlier studies have shown that hypertension-induced cardiac hypertrophy causes an alteration in the amplitude and the time course of systolic  $\text{Ca}^{2+}$  transients. Fowler *et al.*<sup>25</sup> showed that NCX activity is diminished, whereas the amplitude of  $\text{Ca}^{2+}$  transient and SR  $\text{Ca}^{2+}$  content are increased in spontaneously hypertensive rats in comparison with their respective controls. It was suggested that alteration in  $\text{Ca}^{2+}$  signaling during compensated hypertrophy is attributed to the reduction in ventricular myocyte NCX activity. As a result, SR  $\text{Ca}^{2+}$  content increases and thus, the  $\text{Ca}^{2+}$  transient amplitude, serving to maintain the force of contraction against the elevated afterload<sup>25,45</sup>. This observation is consistent with the increased SR  $\text{Ca}^{2+}$  content of spontaneously hypertensive rat ventricular cells reported previously<sup>46</sup>. Similarly, an increase in SR  $\text{Ca}^{2+}$  content, SR  $\text{Ca}^{2+}$  release and amplitude of  $\text{Ca}^{2+}$  transients were also described in a canine model of compensated hypertrophy that was induced by chronic atrioventricular block<sup>47</sup>.

Earlier studies have also reported that abnormal intracellular  $\text{Ca}^{2+}$  transport is caused by the change in expression of proteins that modulate intracellular  $\text{Ca}^{2+}$ . For example, Teshima *et al.*<sup>23</sup> showed that expression of SERCA and RyR mRNA were significantly altered in the heart, 3 and 12 weeks post-STZ injection, respectively. Hattori *et al.*<sup>7</sup> showed that the reduction in cardiac NCX activity is due to the reduction in

NCX mRNA and protein 6 weeks after the induction of diabetes with STZ. Changes in the expression of mRNA that encodes different proteins in cardiac muscle have also been previously reported in data from our laboratory<sup>48</sup>.

Transmural gradients in myocyte  $\text{Ca}^{2+}$  handling proteins exist across the ventricular wall. For example, it has been shown that  $\text{Ca}^{2+}$  handling proteins, such as SERCA, RyR and NCX, are more abundant in the EPI cells than ENDO cells in various species<sup>49–51</sup>. The results of the present study showed that the amplitude of the NCX current is larger in EPI-CON compared with END-CON. Supporting this finding, Xiong *et al.*<sup>51</sup> reported that the NCX current, protein and mRNA were greater in EPI than ENDO or midmyocardial cells. Wang *et al.*<sup>20</sup> also reported the transmural gradient in NCX with the capacity for  $\text{Ca}^{2+}$  extrusion by NCX being ENDO < midmyocardial < EPI. The spatial electrical heterogeneity of ion channels and proteins has a profound effect not only on normal cardiac electrophysiology and contractility, but also on the genesis of cardiac arrhythmias in diseased hearts. For example, the loss of this non-uniformity has been previously reported to be a sensitive index to discriminate physiological from pathological left ventricular remodeling<sup>21</sup>. The diminished NCX function in diabetic myocytes shown in the present study suggest that NCX function might play an important role when  $\text{Ca}^{2+}$  rises to pathological levels, such as in diabetic cardiomyopathy. Furthermore, the disruption of the transmural NCX gradient in diabetic heart highlights a potential substrate for the production of lethal arrhythmias leading to heart failure in diabetes patients.

In conclusion, the present study suggests that STZ-induced diabetes causes a significant rise in  $\text{Ca}^{2+}$  transient amplitudes 5–6 weeks after the induction of diabetes with a single intraperitoneal injection of STZ. This change probably stems partly from the dysfunction of NCX. Additional studies would be required to further our understanding of how diabetes alters  $\text{Ca}^{2+}$  handling in different regions of the heart. This will contribute to the development of new and regionally targeted treatments for diabetic cardiomyopathy.

## ACKNOWLEDGMENTS

The work was funded by the College of Medicine and Health Sciences, UAE University in Al Ain; Zayed University in Abu Dhabi; and Al Ain Equestrian, Shooting and Golf Club.

## DISCLOSURE

The authors declare no conflict of interest.

## REFERENCES

1. Eisner DA, Caldwell JL, Kistamas K, *et al.* Calcium and excitation-contraction coupling in the heart. *Circ Res* 2017; 121: 181–195.
2. Bodi I, Mikala G, Koch SE, *et al.* The L-type calcium channel in the heart: the beat goes on. *J Clin Invest* 2005; 115: 3306–3317.

3. Walsh C, Barrow S, Voronina S, *et al.* Modulation of calcium signalling by mitochondria. *Biochim Biophys Acta* 2009; 1787: 1374–1382.
4. Shao CH, Rozanski GJ, Patel KP, *et al.* Dyssynchronous (non-uniform) Ca<sup>2+</sup> release in myocytes from streptozotocin-induced diabetic rats. *J Mol Cell Cardiol* 2007; 42: 234–246.
5. Howarth FC, Almugaddum FA, Qureshi MA, *et al.* The effects of heavy long-term exercise on ventricular myocyte shortening and intracellular Ca<sup>2+</sup> in streptozotocin-induced diabetic rat. *J Diabetes Complications* 2010; 24: 278–285.
6. Ren J, Walsh MF, Hamaty M, *et al.* Altered inotropic response to IGF-I in diabetic rat heart: influence of intracellular Ca<sup>2+</sup> and NO. *Am J Physiol* 1998; 275: H823–H830.
7. Hattori Y, Matsuda N, Kimura J, *et al.* Diminished function and expression of the cardiac Na<sup>+</sup>-Ca<sup>2+</sup> exchanger in diabetic rats: implication in Ca<sup>2+</sup> overload. *J Physiol* 2000; 527(Pt 1): 85–94.
8. Lee TI, Chen YC, Kao YH, *et al.* Rosiglitazone induces arrhythmogenesis in diabetic hypertensive rats with calcium handling alteration. *Int J Cardiol* 2013; 165: 299–307.
9. Lagadic-Gossmann D, Buckler KJ, Le Prigent K, *et al.* Altered Ca<sup>2+</sup> handling in ventricular myocytes isolated from diabetic rats. *Am J Physiol* 1996; 270(5 Pt 2): H1529–H1537.
10. Takeda N, Dixon IM, Hata T, *et al.* Sequence of alterations in subcellular organelles during the development of heart dysfunction in diabetes. *Diabetes Res Clin Pract* 1996; 30 (Suppl): 113–122.
11. Choi KM, Zhong Y, Hoit BD, *et al.* Defective intracellular Ca (2+) signaling contributes to cardiomyopathy in Type 1 diabetic rats. *Am J Physiol Heart Circ Physiol* 2002; 283: H1398–H1408.
12. Hamouda NN, Sydorenko V, Qureshi MA, *et al.* Dapagliflozin reduces the amplitude of shortening and Ca(2+) transient in ventricular myocytes from streptozotocin-induced diabetic rats. *Mol Cell Biochem* 2015; 400: 57–68.
13. Chattou S, Diacono J, Feuvray D. Decrease in sodium-calcium exchange and calcium currents in diabetic rat ventricular myocytes. *Acta Physiol Scand* 1999; 166: 137–144.
14. Shao CH, Wehrens XH, Wyatt TA, *et al.* Exercise training during diabetes attenuates cardiac ryanodine receptor dysregulation. *J Appl Physiol* 1985; 2009: 1280–1292.
15. Tian C, Shao CH, Moore CJ, *et al.* Gain of function of cardiac ryanodine receptor in a rat model of type 1 diabetes. *Cardiovasc Res* 2011; 91: 300–309.
16. Rithalia A, Qureshi MA, Howarth FC, *et al.* Effects of halothane on contraction and intracellular calcium in ventricular myocytes from streptozotocin-induced diabetic rats. *Br J Anaesth* 2004; 92: 246–253.
17. Howarth FC, Qureshi MA. Effects of carbenoxolone on heart rhythm, contractility and intracellular calcium in streptozotocin-induced diabetic rat. *Mol Cell Biochem* 2006; 289: 21–29.
18. Remme CA, Verkerk AO, Hoogaars WM, *et al.* The cardiac sodium channel displays differential distribution in the conduction system and transmural heterogeneity in the murine ventricular myocardium. *Basic Res Cardiol* 2009; 104: 511–522.
19. Abd Allah ES, Aslanidi OV, Tellez JO, *et al.* Postnatal development of transmural gradients in expression of ion channels and Ca<sup>2+</sup>-handling proteins in the ventricle. *J Mol Cell Cardiol* 2012; 53: 145–155.
20. Wang W, Gao J, Entcheva E, *et al.* A transmural gradient in the cardiac Na/K pump generates a transmural gradient in Na/Ca exchange. *J Membr Biol* 2010; 233: 51–62.
21. Ait Mou Y, Reboul C, Andre L, *et al.* Late exercise training improves non-uniformity of transmural myocardial function in rats with ischaemic heart failure. *Cardiovasc Res* 2009; 81: 555–564.
22. Lu Z, Jiang YP, Xu XH, *et al.* Decreased L-type Ca<sup>2+</sup> current in cardiac myocytes of type 1 diabetic Akita mice due to reduced phosphatidylinositol 3-kinase signaling. *Diabetes* 2007; 56: 2780–2789.
23. Teshima Y, Takahashi N, Saikawa T, *et al.* Diminished expression of sarcoplasmic reticulum Ca(2+)-ATPase and ryanodine sensitive Ca(2+)Channel mRNA in streptozotocin-induced diabetic rat heart. *J Mol Cell Cardiol* 2000; 32: 655–664.
24. McCrossan ZA, Billeter R, White E. Transmural changes in size, contractile and electrical properties of SHR left ventricular myocytes during compensated hypertrophy. *Cardiovasc Res* 2004; 63: 283–292.
25. Fowler MR, Naz JR, Graham MD, *et al.* Decreased Ca<sup>2+</sup> extrusion via Na<sup>+</sup>/Ca<sup>2+</sup> exchange in epicardial left ventricular myocytes during compensated hypertrophy. *Am J Physiol Heart Circ Physiol* 2005; 288: H2431–H2438.
26. Casis O, Gallego M, Iriarte M, *et al.* Effects of diabetic cardiomyopathy on regional electrophysiologic characteristics of rat ventricle. *Diabetologia* 2000; 43: 101–109.
27. Smail MM, Qureshi MA, Shmygol A, *et al.* Regional effects of streptozotocin-induced diabetes on shortening and calcium transport in epicardial and endocardial myocytes from rat left ventricle. *Physiol Rep* 2016; 4: e13034.
28. Al Kury L, Sydorenko V, Smail MMA, *et al.* Voltage dependence of the Ca(2+) transient in endocardial and epicardial myocytes from the left ventricle of Goto-Kakizaki type 2 diabetic rats. *Mol Cell Biochem* 2018; 446: 25–33.
29. Szkudelski T. Streptozotocin-nicotinamide-induced diabetes in the rat. Characteristics of the experimental model. *Exp Biol Med* 2012; 237: 481–490.
30. Cheta D. Animal models of type I (insulin-dependent) diabetes mellitus. *J Pediatr Endocrinol Metab* 1998; 11: 11–19.
31. Al Kury LT, Yang KH, Thayyullathil FT, *et al.* Effects of endogenous cannabinoid anandamide on cardiac Na(+)/Ca(2+)(+) exchanger. *Cell Calcium* 2014; 55: 231–237.



32. Bracken N, Howarth FC, Singh J. Effects of streptozotocin-induced diabetes on contraction and calcium transport in rat ventricular cardiomyocytes. *Ann N Y Acad Sci* 2006; 1084: 208–222.
33. Yaras N, Ugur M, Ozdemir S, *et al.* Effects of diabetes on ryanodine receptor Ca release channel (RyR2) and Ca<sup>2+</sup> homeostasis in rat heart. *Diabetes* 2005; 54: 3082–3088.
34. Arikawa M, Takahashi N, Kira T, *et al.* Enhanced inhibition of L-type calcium currents by troglitazone in streptozotocin-induced diabetic rat cardiac ventricular myocytes. *Br J Pharmacol* 2002; 136: 803–810.
35. Moore CJ, Shao CH, Nagai R, *et al.* Malondialdehyde and 4-hydroxynonenal adducts are not formed on cardiac ryanodine receptor (RyR2) and sarco(endo)plasmic reticulum Ca<sup>2+</sup>-ATPase (SERCA2) in diabetes. *Mol Cell Biochem* 2013; 376: 121–135.
36. Hamouda NN, Qureshi MA, Alkaabi JM, *et al.* Reduction in the amplitude of shortening and Ca(2+) transient by phlorizin and quercetin-3-O-glucoside in ventricular myocytes from streptozotocin-induced diabetic rats. *Physiol Res* 2016; 65: 239–250.
37. Yaras N, Bilginoglu A, Vassort G, *et al.* Restoration of diabetes-induced abnormal local Ca<sup>2+</sup> release in cardiomyocytes by angiotensin II receptor blockade. *Am J Physiol Heart Circ Physiol* 2007; 292: H912–H920.
38. Lee MJ, Lee HS, Park SD, *et al.* Leonurus sibiricus herb extract suppresses oxidative stress and ameliorates hypercholesterolemia in C57BL/6 mice and TNF- $\alpha$  induced expression of adhesion molecules and lectin-like oxidized LDL receptor-1 in human umbilical vein endothelial cells. *Biosci Biotechnol Biochem* 2010; 74: 279–284.
39. Lacombe VA, Viatchenko-Karpinski S, Terentyev D, *et al.* Mechanisms of impaired calcium handling underlying subclinical diastolic dysfunction in diabetes. *Am J Physiol Regul Integr Comp Physiol* 2007; 293: R1787–R1797.
40. Zhang L, Ward ML, Phillips AR, *et al.* Protection of the heart by treatment with a divalent-copper-selective chelator reveals a novel mechanism underlying cardiomyopathy in diabetic rats. *Cardiovasc Diabetol* 2013; 12: 123.
41. Kohajda Z, Farkas-Morvay N, Jost N, *et al.* The effect of a novel highly selective inhibitor of the sodium/calcium exchanger (NCX) on cardiac arrhythmias in *in vitro* and *in vivo* experiments. *PLoS One* 2016; 11: e0166041.
42. Howarth FC, Adem A, Adeghate EA, *et al.* Distribution of atrial natriuretic peptide and its effects on contraction and intracellular calcium in ventricular myocytes from streptozotocin-induced diabetic rat. *Peptides* 2005; 26: 691–700.
43. Gilca GE, Stefanescu G, Badulescu O, *et al.* Diabetic cardiomyopathy: current approach and potential diagnostic and therapeutic targets. *J Diabetes Res* 2017; 2017: 1310265.
44. Bidasee KR, Nallani K, Yu Y, *et al.* Chronic diabetes increases advanced glycation end products on cardiac ryanodine receptors/calcium-release channels. *Diabetes* 2003; 52: 1825–1836.
45. Naqvi RU, Macleod KT. Effect of hypertrophy on mechanisms of relaxation in isolated cardiac myocytes from guinea pig. *Am J Physiol*. 1994; 267(5 Pt 2): H1851–H1861.
46. Brooksby P, Levi AJ, Jones JV. Investigation of the mechanisms underlying the increased contraction of hypertrophied ventricular myocytes isolated from the spontaneously hypertensive rat. *Cardiovasc Res* 1993; 27: 1268–1277.
47. Sipido KR, Volders PG, de Groot SH, *et al.* Enhanced Ca(2+) release and Na/Ca exchange activity in hypertrophied canine ventricular myocytes: potential link between contractile adaptation and arrhythmogenesis. *Circulation* 2000; 102: 2137–2144.
48. Salem KA, Qureshi MA, Sydorenko V, *et al.* Effects of exercise training on excitation-contraction coupling and related mRNA expression in hearts of Goto-Kakizaki type 2 diabetic rats. *Mol Cell Biochem* 2013; 380: 83–96.
49. Currie S, Quinn FR, Sayeed RA, *et al.* Selective down-regulation of sub-endocardial ryanodine receptor expression in a rabbit model of left ventricular dysfunction. *J Mol Cell Cardiol* 2005; 39: 309–317.
50. Igarashi-Saito K, Tsutsui H, Takahashi M, *et al.* Endocardial versus epicardial differences of sarcoplasmic reticulum Ca<sup>2+</sup>-ATPase gene expression in the canine failing myocardium. *Basic Res Cardiol* 1999; 94: 267–273.
51. Xiong W, Tian Y, DiSilvestre D, *et al.* Transmural heterogeneity of Na<sup>+</sup>-Ca<sup>2+</sup> exchange: evidence for differential expression in normal and failing hearts. *Circ Res* 2005; 97: 207–209.

## SUPPORTING INFORMATION

Additional supporting information may be found online in the Supporting Information section at the end of the article.

**Appendix S1** | Solutions and reagents.